

Figure 1: Simplified schematic of the compensated lattice setup

1 Compensated optical lattice

Our experiments take place in a compensated simple cubic optical lattice potential, which is formed at the intersection of three orthogonal axes, see Fig. 1. Along each axis, a 1D lattice potential is formed by retro-reflecting a red-detuned Gaussian beam, which results in a sinusoidal intensity pattern.

Overlapped onto each of the lattice beams we have a compensation beam, which is blue-detuned and thus produces a repulsive potential. The compensation beam is not retro-reflected, so it does not form a standing wave potential, see Fig. 1.

The lattice beam that propagates along the x axis produces a potential of the form

$$V_L(x; y, z) = -s_0 \exp\left[-2\frac{y^2 + z^2}{w_L^2}\right] \cos^2(k_L x) \quad (1)$$

where s_0 is the lattice depth at the center of the potential, w_L is the lattice beam waist and $k_L = 2\pi/\lambda_L$ is the wavenumber of the lattice light. The compensation beam that propagates along x produces a potential

$$V_C(x; y, z) = g_0 \exp\left[-2\frac{y^2 + z^2}{w_C^2}\right] \quad (2)$$

where g_0 is the depth (or rather height since it is repulsive) of the compensating potential, and w_C is the beam waist of the compensation beam.

The combined potential of lattice plus compensation for the beams propagating along x is

$$V_{1D}(x; y, z) = V_L(x; y, z) + V_C(x; y, z) \quad (3)$$

The total potential for our simple cubic lattice is given by

$$V_{3D}(x, y, z) = V_{1D}(x; y, z) + V_{1D}(y; z, x) + V_{1D}(z; x, y) \quad (4)$$

In what follows we will study the properties of a two-state spin mixture of fermionic atoms in the compensated optical lattice potential. We will first look at general aspects of the potential, using analytic approximations to its shape and considering a zero temperature sample. Then we will use the high-temperature series expansion (HTSE)¹ and the local density approximation (LDA) to explore the

¹The HTSE is an analytical solution to the Hubbard model that is valid at high-temperatures. The HTSE is very good

properties of the system in more detail.

2 General aspects of the potential

Before we go ahead and deploy the full machinery of the LDA we will discuss some general aspects of the potential.

One of the important things to note is that at each point in space we will, in general, have three different lattice depths, associated with each of the x , y , and z lattice directions. For this reason the potential is difficult to visualize. To make things simpler, we can consider the potential along the 111 direction, along this direction we have equal lattice depths in x , y , and z :

$$s_x(r_{111}) = s_y(r_{111}) = s_z(r_{111}) = s_0 \exp\left[-\frac{4r_{111}^2}{3w_L^2}\right] \equiv s(r_{111}) \quad (5)$$

where r_{111} represents the distance along the 111 diagonal line.

The bottom envelope of the lattice potential along 111 is given by

$$V_{L,\text{env}}(r_{111}) = -3s_0 \exp\left[-\frac{4r_{111}^2}{3w_L^2}\right] \quad (6)$$

An important aspect of a lattice potential is that the energy spectrum exhibits a band structure. The lowest energy of the band, E_0 , measured from the potential envelope $V_{L,\text{env}}$, can be approximated by the zero-point energy of the 3D harmonic oscillator obtained by Taylor expanding the potential at a lattice site. This approximation is only valid for deep lattices ($\gtrsim 10 E_R$) but we will use it here for its simplicity:

$$E_0 = \frac{3}{2}\hbar\omega_0 = 3E_R\sqrt{s/E_R} \quad (7)$$

We can also obtain an expression for the bandwidth W , valid in the limit of deep lattices [1]:

$$W = 12t = E_R \frac{48}{\sqrt{\pi}} (s/E_R)^{3/4} e^{-2\sqrt{s/E_R}} \quad (8)$$

Notice that the quantities E_0 , ω_0 , s , and t are all functions of r_{111} .

The energy of the first excited band in the lattice corresponds to an excitation along one of the lattice directions, which is an extra $\hbar\omega_0$ above the lowest band. In Fig. 2 we have plotted the lattice potential envelopes along with the energy boundaries of the lowest band and a line that is representative of the energy in the first excited band. Also indicated in Fig. 2 is the radius, $r_{1\text{st}}$, at which the energy of the lowest band is equal to the band gap at the origin:

$$E_0(r_{1\text{st}}) = E_1(0) \quad (9)$$

In order to stay within the single band approximation of the Hubbard model, our sample needs to have a size that is smaller than $r_{1\text{st}}$.

for $T \gg t$ and works down to $T/t \sim 1.8$. This solution gives us the thermodynamic quantities (density, double occupancy, entropy per particle, etc.) for a homogeneous system.

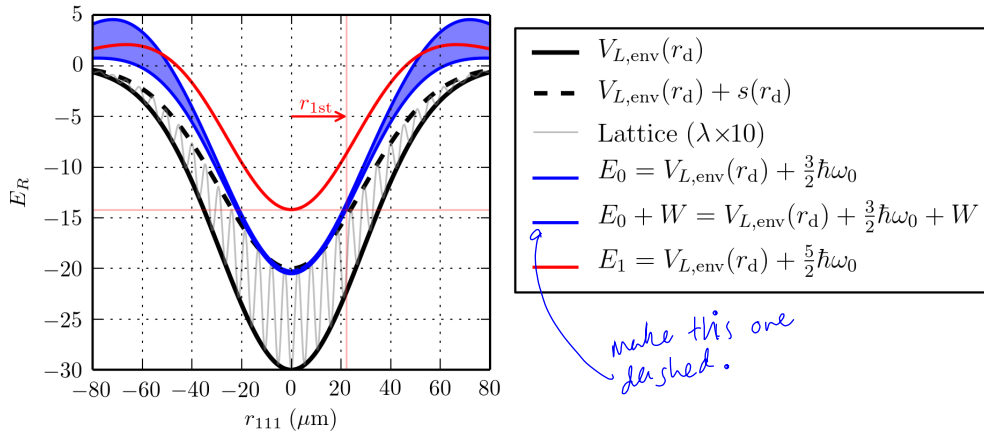


Figure 2: Profiles along r_{111} for a $10E_R$ lattice with $w_L = 47 \mu\text{m}$.

2.1 Lattice locking

On occasion we will want to raise the lattice depth suddenly. This will be useful to get the maximum possible Debye-Waller factor when performing Bragg scattering, or to keep the density distribution frozen when sweeping across the narrow Feshbach resonance to make doublons.

For Feshbach sweeps across the narrow resonance we have found that going across from $80 a_0$ to $61 a_0$ in 24 ms gives us nearly 100% doublon-to-molecule conversion efficiency. For some measurements we blow away any remaining atoms with a resonant light pulse and sweep back across the resonance to dissociate the molecules. For such a procedure we require the density distribution to remain locked for times up to 48 ms. To have less than 0.1 tunneling events in 48 ms, the tunneling rate in the lattice should be less than 2 Hz. *change sentence order.*

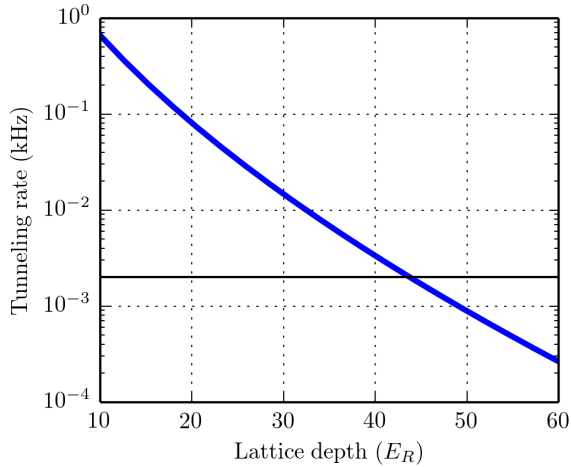
3a On Fig. 3 we show the tunneling rate as a function of lattice depth, and we see that to achieve 2 Hz one needs $s_0 \approx 44 E_R$. With that in mind we have to consider that as we lock-up the lattice to $44 E_R$ we want to stay within the single band Hubbard model. Figure 3 also shows the atom number, N_{1st} , corresponding to a sample with density $n = 1$ atom per site filled up to r_{1st} . For atom numbers greater than N_{1st} the single band approximation breaks down. *3b*

From Fig. 3 we see that for samples of $N = 300,000$ atoms and a lattice beam waist of $47 \mu\text{m}$, the maximum lock depth to stay in the single band regime is $\approx 10 E_R$. Currently, when doing Bragg scattering measurements, we lock the lattice up to $20 E_R$ to get the largest possible Debye-Waller factor. In the Bragg experiment we use a compensation of $3 E_R$ to flatten out a $7 E_R$ lattice and we leave the compensation on during the lattice lock. Having $3 E_R$ of compensation gives us a maximum atom number of $\approx 230,000$ atoms to stay in the single band regime, as is shown with the dotted line in Fig. 3.b)

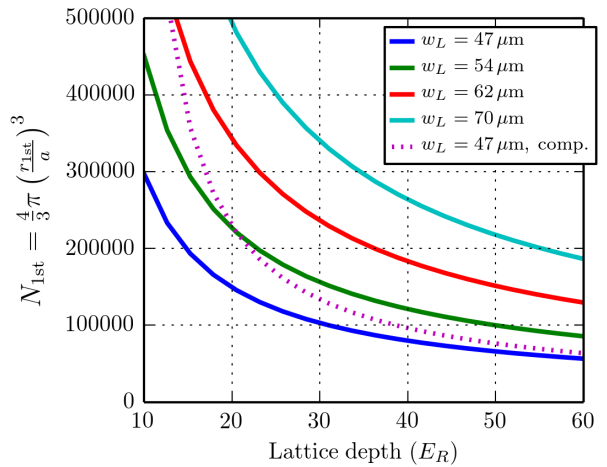
Our latest experiments with Bragg scattering use an atom number $N \approx 300,000$, so we are putting ourselves slightly outside of the single band regime. We have observed that locking the lattice to deeper values, such as $50 E_R$ and $80 E_R$ deteriorates our Bragg signals. This is, perhaps, due to the inability to stay in the single band regime when locking our sample to such depths with the number of atoms that we have. *Besides exciting atoms to higher bands with the odder*

For the measurement of the double occupancy, we have found that Feshbach molecules scatter green light strongly. If we shine any green light on them, we lose them in just a few milliseconds. This means that, when considering doublon measurements, we cannot afford to have any green compensation light

parameter will be smaller for parts of the trap which can also affect Bragg depth, the effective Lamb-Dicke



(a) Tunneling rate. The black line is at 2 Hz, which is the rate required to keep the lattice frozen during a measurement of the double occupancy.



(b) Maximum atom number to stay in the single band regime. The dashed line includes $3 E_R$ of compensation, with a compensation beam waist of $w_C = 40 \mu\text{m}$.

Figure 3: Atom number constraints when locking the lattice.

on. With this in mind we see from Fig. 3 that, in order to lock the lattice up to $44 E_R$ and have the capacity to hold $N \approx 250,000$ in the single band regime, we would require a lattice beam waist as large as $70 \mu\text{m}$.

Our current lattice waist of 47 μm is an important limitation for our ability to enhance the Debye-Waller factor for Bragg scattering or to freeze tunneling to measure

We are interested in exploring the idea of evaporative cooling in a lattice and also the concept of the entropy capacity of the lattice system. We will see that for both these two ideas it will be necessary to introduce the concept of compensation. Compensation is a way of flattening the profile of the lowest band in order to enlarge the central region of the sample which may exhibit the phase of interest.

We will see that using small lattice beam waists and compensation may lead to evaporative cooling in the lattice potential.

With the addition of repulsive compensation beams with depth g_0 and beam waist w_C , as in Eq. 2, we can expand the lowest band profile of the lattice in a power series as

$$E_0(r_{111}) \approx 3(g_0 + E_R \sqrt{s_0/E_R} - s_0) + \left[\frac{4s_0 - 2E_R \sqrt{s_0/E_R}}{w_L^2} - \frac{4g_0}{w_C^2} \right] r_{111}^2 + \left[\frac{-8s_0 + 2E_R \sqrt{s_0/E_R}}{3w_L^4} + \frac{8g_0}{3w_C^4} \right] r_{111}^4 + \mathcal{O}(r_{111}^6) \quad (10)$$

Enlarging the Mott plateau If our interest is to maximally flatten the band profile, we see that we can completely cancel the quadratic term in the series expansion by choosing

$$g_0 = \frac{4s_0 - 2\sqrt{s_0}}{4\alpha_w^2} \equiv g_{\text{quartic}} \quad (11)$$

where we define the beam waist ratio $\alpha_w = w_L/w_C$ as in [4]. This choice of g_0 will be the most favorable in enlarging the size of the $n = 1$ region of the cloud.

We point out that, for $\alpha_w > 1$, if we use a compensation larger than g_{quartic} , the band profile would have a bump in the center. We have observed experimentally that in that case it becomes hard to align

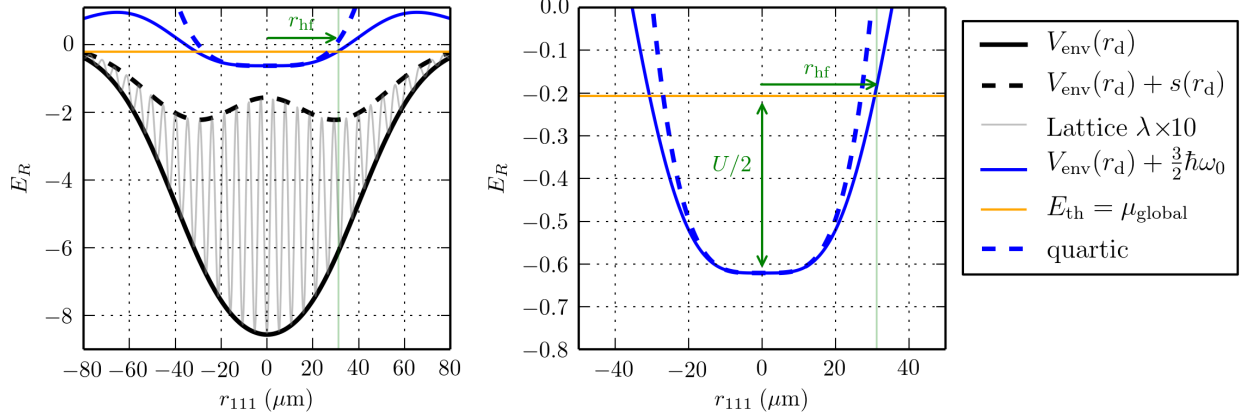


Figure 4: Profiles along r_{111} for a $7 E_R$ lattice with $w_L = 47 \mu\text{m}$. The compensation is $g_0 = g_{\text{quartic}}$, and the chemical potential is set at $U/2$ to achieve half-filling. This conditions determine the waist ratio $\alpha_{w,\text{evap}} = 1.17$ such that the chemical potential also matches the evaporation threshold. The figure on the left shows the profile of the lattice potential, which illustrates how the energy scales of the potentials are significantly larger than the energy scales of the Fermi-Hubbard parameters U and t . The figure on the right is a zoomed in version of the one on the left.

the compensation beams such that the sample actually stays at the center of the trap.

In our current experiments we use $s_0 = 7 E_R$ and our beam waists are approximately $w_L = 47 \mu\text{m}$ and $w_C = 40 \mu\text{m}$, which gives $\alpha_w = 1.175$. The necessary compensation to flatten the band would be $g_{\text{quartic}} = 4.11 E_R$

Evaporation. We want to consider the possibility of evaporative cooling in a sample that has $n = 1$ at the center. To impose this half-filling condition we need to set the global chemical potential, μ_{global} (measured from the lowest point along the band profile), at a value $U/2$, where U is the on-site interaction strength. This prescription to obtain half-filling is obtained from the HTSE solution to the homogeneous Fermi-Hubbard model.

At zero temperature, μ_{global} can be obtained as the value of the band profile at the radius that defines the edge of the cloud. In this way, the half-filling requirement can be written as

$$\mu_{\text{global}} = E_0(r_{\text{hf}}) - E_0(0) = U/2 \quad (12)$$

which defines the radius of the half-filled sample, r_{hf} . The situation is illustrated in Fig. 4.

In order to maximize the evaporation rate for a half-filled sample we need $E_0(r_{\text{hf}})$ to come as close as possible to the evaporation threshold energy, E_{th} . In our setup the threshold is the energy required to escape along one of the lattice beams:

$$E_{\text{th}} = g_0 + E_R \sqrt{s_0/E_R} - s_0 = \frac{E_0(0)}{3} \quad 3E_{\text{TH}} = E_0(0) \quad (13)$$

The best we can do is set $E_{\text{th}} = E_0(r_{\text{hf}})$ which, along with Eq. 12, results in

$$\frac{E_0(0)}{3} = \frac{U}{2} + E_0(0) \quad -2(g_0 + E_R \sqrt{s_0/E_R} - s_0)E_R = U/2$$

To maximize the size of the Mott plateau we set $g_0 = g_{\text{quartic}}$, and then we solve for the beam waist

$$-\frac{2}{3}E_0(0) = \frac{U}{2} \Rightarrow$$

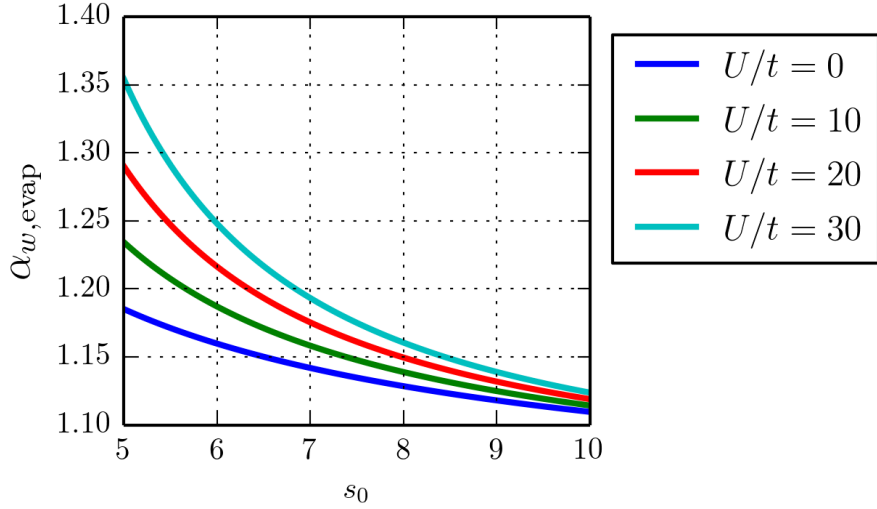


Figure 5: Optimal beam waist ratio for enlarging the central flat portion on the band and maximizing the rate of evaporative cooling.

ratio $\alpha_{w,\text{evap}}$, which optimizes the evaporation rate in the lattice:

$$\alpha_{w,\text{evap}}^2 = \frac{4s_0 - 2E_R\sqrt{s_0/E_R}}{4s_0 - 4E_R\sqrt{s_0/E_R} - U} \quad (15)$$

For a deep lattice ($\gtrsim 10 E_R$) the on-site interactions can be expressed analytically as

$$\frac{U}{E_R} = 4\sqrt{2\pi} \frac{a_s}{\lambda} (s/E_R)^{3/4} \quad (16)$$

The scattering length is usually expressed in units of the Bohr radius, a_0 , so it is useful to keep in mind that for our 1064 nm lattice $\lambda = 20113 a_0$. In our experiment we want to avoid very large scattering lengths because they give rise to fast inelastic losses that scale as a_s^4 ; reasonable values of a_s are up to $800 a_0$. In a $7 E_R$ lattice a scattering length $a_s = 800 a_0$ implies an interaction strength $U/t = 35$, calculated from Eq. 16. In Fig. 5 we show plots of $\alpha_{w,\text{evap}}$ for various values of U/t .

we can have a most favorable situation for evaporative cooling if
We can see from Fig. 5 that for a $7 E_R$ lattice, $\alpha_{w,\text{evap}}$ is between 1.15 and 1.20. This optimal-evaporation beam waist ratio is obtained for $g_0 = g_{\text{quartic}}$ so the size of the Mott plateau is maximized.

In conclusion, a compensated lattice with $U/t = 1.7$ offers the best scenario for evaporation while flattening the bottom of the band.

Atom number We now turn to examine the number of atoms required in order to achieve half-filling in the optimal setup. To get this number we need to find the half-filling radius, r_{hf} , which is defined by Eqs. 12 and 13. Using a density of one atom per site we can find the atom number from the radius, as $N_{\text{hf}} = \frac{4}{3}\pi(r_{\text{hf}}/a)^3$, where a is the lattice spacing ($a = \lambda/2$).

To solve Eqs. 12 and 13 we can use the power series expansion of the band energy, which for $g_0 = g_{\text{quartic}}$ is

$$E_0(r_{111}) - E_0(0) = \left[\frac{2E_R\sqrt{s_0/E_R} - 8s_0 + 4(2s_0 - E_R\sqrt{s_0/E_R})\alpha_w^4}{3w_L^4} \right] r_{111}^4 \quad (17)$$

N will be too large so far w[↑] α_w^{-1}

At the

The solution for r_{hf} is then

fig of went: sample > n=1

$$r_{\text{hf}} = \frac{w_L}{\alpha_w} \left[\frac{3(1 - 2\alpha_w^4 + 2\sqrt{s_0/E_R}(\alpha_w^4 - 1))}{2(1 - 2\alpha_w^4 + 4\sqrt{s_0/E_R}(\alpha_w^4 - 1))} \right]^{1/4}$$

will give the same number. Number in the phase is smaller.

For $s_0 = 7$ and $\alpha_w = 1.17$ this gives $r_{\text{hf}} \approx 0.7w_L$. For a lattice beam waist $w_L = 47 \mu\text{m}$ this amounts to $N_{\text{hf}} = 990,000$ atoms. The fully optimized situation for $w_L = 47 \mu\text{m}$ is shown in Fig. 4.

Considerations for our current setup In our current setup we use a lattice depth $s_0 = 7 E_R$, and we have approximately $w_L = 47 \mu\text{m}$ and $w_C = 40 \mu\text{m}$, which amounts to $\alpha_w = 1.175$. As we have seen above, we should compensate this sample with $g_{\text{quartic}} = 4.11 E_R$ and populate it with $N \approx 990,000$ atoms. This would yield a half-filled sample with optimal conditions for evaporative cooling in the lattice.

Unfortunately we only have $\approx 300,000$ atoms at our disposal. This forces us to reduce the compensation below g_{quartic} in order to achieve $n = 1$ at the center. Reducing the compensation significantly affects the prospects of evaporative cooling in the lattice. *A more quantitative study will be presented later on with the full machinery of the LDA.*

At the moment we use the following compensations for each of the three axes:

axis	1	2	3
g_0	3.65	3.90	2.9

With these values we have found empirically that we can obtain the same confinement frequencies in all three directions (which produces spherically symmetric samples) and that we can achieve $n = 1$ at the center with $N \approx 300,000$ atoms.

Why is our atom number 300,000? At the moment our experimental sequence consists of the following steps:

1. Evaporate into a dimple potential with a depth of $\approx 0.5 E_R$ per axis. The cold sample in the dimple has a density of nearly one atom per site.
2. Rotate the polarization of the retro beams to go from dimple to lattice configuration. We want the sample in the dimple to have a Fermi energy $E_F < E_R$ so that we can be sure that all of the atoms will remain in the lowest band as we rotate to a lattice potential. While we rotate we add a minimal amount of compensation, $0.06 E_R$.
3. Ramp up the lattice depth in 25 ms up to the point where the lowest band and first excited band separate, which corresponds to a lattice depth of $\approx 2.4 E_R$. At the same time add $0.65 E_R$ of compensation. During this time also ramp the interaction strength from the evaporation value to the value we want in the experiment.
4. Ramp up, in 15 ms, the lattice depth to $7 E_R$ and the compensation to the desired final value.

So far in our experiments we have tried to keep the density at one per site from the moment we start in the dimple at Step 1, up to the final sample in the lattice. Keeping the density at $n = 1$ gives us a constraint for the number of atoms that we start with in the dimple potential. We derive this below.

In the dimple, having a peak density of one per site translates into having a global trap Fermi energy which is $E_{F,\text{trap}} \approx E_R$. *In fact, the local Fermi energy at the center of the trap and the density there can be related by $E_F = \frac{\hbar}{2m}(3\pi^2n)^{2/3}$.* Setting the density to one per site, $n = a^{-3}$ yields

$E_F = (3/\pi)^{2/3} E_R \approx 0.97 E_R$. The local Fermi energy at the center will be the same as the global Fermi energy of the harmonic trap, so we can find the total trapped atom number from

$$E_{F,\text{trap}} = \hbar\omega(3N)^{1/3} = E_R \quad \Rightarrow \quad N = \frac{1}{3} \left(\frac{E_R}{\hbar\omega} \right)^3 \quad (19)$$

A dimple potential with depth V_0 per axis has a trapping frequency

$$\omega = \left(\frac{8V_0}{mw_L^2} \right)^{1/2} = \frac{a\sqrt{2E_R}}{\hbar\pi} \left(\frac{8V_0}{w_L^2} \right)^{1/2} = \frac{4a}{\hbar\pi w_L} (E_R V_0)^{1/2} \quad (20)$$

so

$$N = \frac{1}{3} \left(\frac{\pi w_L}{4a} \right)^3 \left(\frac{E_R}{V_0} \right)^{3/2} \quad (21)$$

With $V_0 = 0.5 E_R$ and $w_L = 47 \mu\text{m}$ we obtain $N = 315,000$ atoms.

Just notice that for this calculation to make sense, the depth of the dimple potential has to be larger than the Fermi energy in the harmonic trap, that is

$$2V_0 > E_{F,\text{trap}} \quad (22)$$

In our setup we just match this condition since $2V_0 = 1 E_R$ and $E_{F,\text{trap}} = 1 E_R$.

Can we load more atoms into the lattice? In order to load more atoms into the lattice we would have to start with a larger number of atoms in the dimple. If we were to initially load a deeper dimple then, for our beam waists, the sample would have a density larger than one per site at the center. This poses a problem because the Fermi energy would be larger than $1 E_R$, and it would lead to population of the first excited band when rotating into the lattice. Furthermore we do not know if we can achieve as low temperatures as we do in the $0.5 E_R$ dimple.

A simple way to circumvent the higher band issue would be to compensate the dimple before rotating the polarization of the retro beams. In that way, a larger atom number can be accommodated at a density of one atom per site, and we could proceed with the ramps that maintain the density at that value. With a larger atom number we would find that we would require a larger g_0 , closer to g_{quartic} , in order to get to half-filling in the final sample.

Why do we stick with 300,000 atoms? We go back to the first consideration of this section: locking the lattice. If we load a sample of more than $N = 230,000$ atoms, the lattice lock to $20 E_R$ compromises our measurement by forcing atoms into the first excited band. Already at our atom number of $N \approx 300,000$ the lock to $20 E_R$ poses somewhat of a compromise, but we have observed Bragg signals there so we are keeping it like it is.

Considerations for future improvements. The main bottleneck for our setup at the moment is related to the lock. A lattice beam waist of $w_L = 70 \mu\text{m}$ would allow us to lock up to $35 E_R$ with a sample of $N = 300,000$ atoms. We will show with the exact calculations of the LDA, that when the atom number is a constraint one can obtain a better scenario for evaporative cooling by using a lower value of α_w . We will see there that a value of $\alpha_w \approx 1.05$, with nearly equal beam waists for lattice and compensation, may be what we want to do.

In the next section we will use the more quantitative LDA results to gain more insight into the compensated lattice setup and help us decide on the best parameters for the future improvements of our setup.

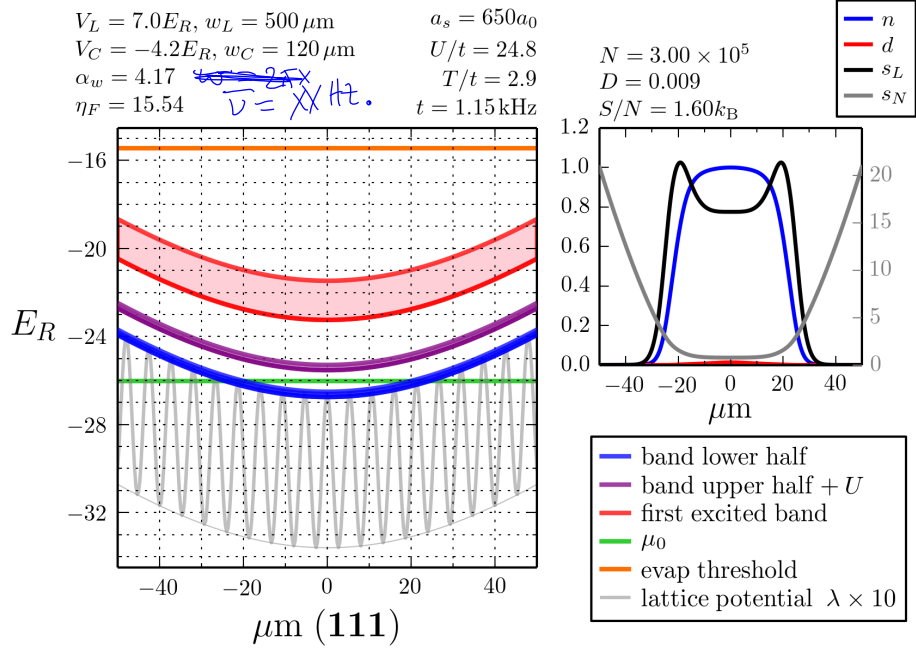


Figure 6: Red detuned uniform lattice with additional harmonic confinement. The confinement is adjusted so that the density is one per site at the center with $N = 300,000$ atoms. The temperature is adjusted such that the overall entropy per particle is $S/N = 1.6k_{\text{B}}$.

3 Local density approximation

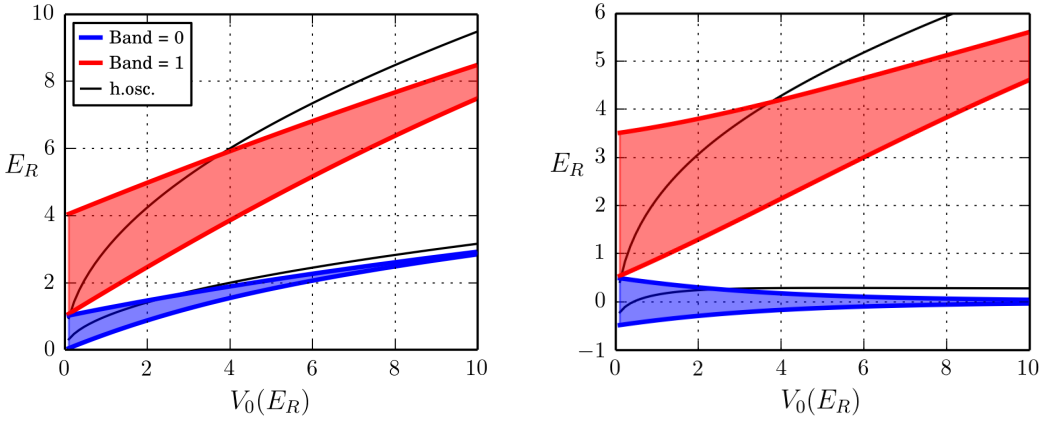
In the local density approximation (LDA) we consider each point in our potential as an homogeneous system and we set the condition that all of these local homogeneous systems are in thermal equilibrium with each other at some temperature T . At each point in our potential we can obtain a local value of the lattice depth and the on-site interactions. These two quantities determine the local values of the Hubbard parameters t and U . With these in hand, we can use a known solution to the homogeneous Hubbard model and obtain local values for the thermodynamic quantities, such as density, double occupancy, entropy, etc. We can plot the local thermodynamic quantities as a function of trap position and obtain trap profiles.

An example of the LDA for a uniform lattice potential plus harmonic confinement is shown in Fig. 6. Notice that to obtain the uniform lattice plus confinement we use large values of the beam waists for the lattice and compensation beams, and we use a negative depth for the compensation beam. The resulting trap frequencies in this setup are $\omega = 342 \text{ Hz}$ in all three directions, calculated for lithium-⁶Li with $m = 6 \text{ AMU}$.

In plots like the one in Fig. 6 we show several lines and regions, and also there are several labels at the top. Below we give the explanation for each of the lines and labels that appear.

Parameters of the potential. The labels on the top left indicate the depth of the lattice and compensating potentials in recoils, and also the waists used for the lattice and compensating beams. The general geometry of the potential is described in §1. Also shown is the beam waist ratio, α_w . The figure of merit for evaporation, η_F will be explained below.

The confinement frequency is equivalent from the curvature of the bottom of the lowest band. at the confinement frequency.



(a) Band structure when the zero of energy is at the bottom of the lattice sites. The zero of energy does not change with lattice depth, and the band energies go up almost like the harmonic oscillator state in an individual lattice site.

(b) Band structure when the zero of energy is at the center of the lowest band. This shift is implicit when the hamiltonian is written in second quantized form as in Eq. 24.

Figure 7: Band structure in the Hubbard model.

Hubbard parameters. The labels on the top right of the main plot indicate the scattering length and the resulting Hubbard parameters for the given lattice depth. The values of U/t , T/t , and t given are valid at the center of the sample. Due to the finite lattice beam waist the tunneling increases as one moves away from the center and so U/t and T/t decrease monotonically for larger distance from the center.

Band lower half. This region is defined by two lines, the bottom line corresponds to the lowest energy level accessible to a single particle in the local Hubbard hamiltonian. The top line corresponds to the energy level exactly in the center of the lowest energy band. In the absence of interactions, the Hubbard hamiltonian for a single particle is simply

$$H = -\frac{\hbar^2}{2m} \frac{\partial}{\partial x^2} + V_0 \sin^2(kx) \quad (23)$$

The energy level structure as a function of lattice depth is as shown in Fig 7a. In second quantized form the hamiltonian (without interactions) is usually written as

$$H = -t \sum_{\langle ij \rangle, \sigma} a_{i\sigma}^\dagger a_{j\sigma} \quad (24)$$

What is typically not mentioned is that writing the hamiltonian as in Eq. 24 implies a lattice-depth-dependent shift of the energy zero, such that the band structure looks like in Fig. 7b. When solving the Hubbard model using the HTSE we used the hamiltonian in Eq. 24, so energies like the chemical potential are referenced from the center of the lowest band. Most importantly, the center of the lowest band is a ubiquitous energy in the Hubbard model because states below that energy will be almost unperturbed by interactions, whereas states above that energy will be affected significantly by interactions.

Band upper half + U . As we just pointed out in the last paragraph, the states above the center of the lowest band will be modified significantly by the interactions. These states will acquire an extra

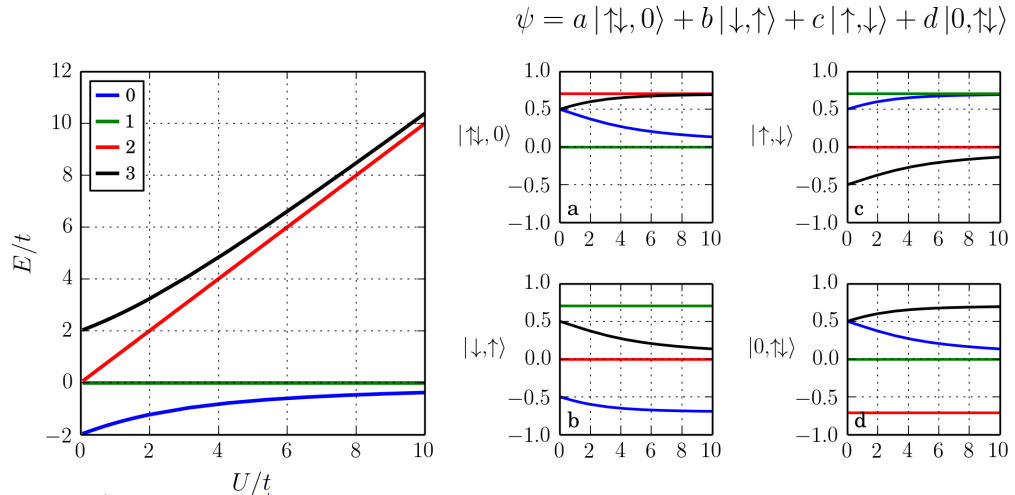


Figure 8: Exact diagonalization solution for the Hubbard hamiltonian, Eq. 25, at half-filling. Notice that the ~~ground state~~ here are second quantized states, so they are already antisymmetrized. For large U the ground state wavefunction is approximately $\psi = \frac{1}{\sqrt{2}}(|\uparrow,\downarrow\rangle - |\downarrow,\uparrow\rangle)$. This state cannot be written down as a Slater determinant because it is an entangled state. For a large number of particles the massive entanglement in the ground state is what makes strongly correlated systems hard to deal with.

energy U , this can be seen for instance if we solve the Hubbard model

$$H = -t \sum_{\langle ij \rangle, \sigma} a_{i\sigma}^\dagger a_{j\sigma} + U \sum_i n_{i\uparrow} n_{i\downarrow} \quad (25)$$

in a two-lattice system at half-filling. The solution to this hamiltonian, using exact diagonalization is shown in Fig. 8. It can be seen that the two lower energy levels suffer ~~almost no~~ little change as the interactions are increased, whereas the two higher energy levels are shifted upwards by U .

The region in the plot called **band upper half + U** represents the energy levels in the upper half of the lowest band shifted up by the interactions. Of course, this simple picture is not correct in the interacting many-body system but it provides a good representation of what is going ~~on~~^{on}. The separation U between the band lower half and the band upper half can be used as a measure of the Mott gap.

First excited band. This region is simply bounded by the lowest and highest energies in the first excited band. For this band we do not apply shifts due to interactions. This band is primarily shown so that, at a glance, one can assess whether or not the system is in the single band Hubbard regime.

Global chemical potential. Denoted by μ_0 . A fixed chemical potential is set across the cloud. ~~For the solutions to the Hubbard model,~~ ^{The} local chemical potential is obtained by looking at the separation between μ_0 and the local zero of energy. We remind the reader that the local zero of energy is the point at the center of the lowest band, i.e. the upper boundary of the blue shaded region.

Evaporation threshold. This is the energy required to escape along one of the lattice beams. It is calculated by looking at the lowest energy level along the 100 direction and getting the largest value. In most cases the largest value is at infinity, but for a compensation beam waist larger than the lattice maximum

beam waist, the lowest energy profile along 100 can have a local maximum. In such cases the local maximum is used.

Figure of merit for evaporative cooling in the lattice (η_F). When evaporative cooling a thermal gas of atoms, one considers the parameter $\eta = U_{\text{trap}}/k_B T$, where T is the temperature of the gas, and U_{trap} is the energy threshold for a particle leaving the trap (i.e. the trap depth) measured with respect to the lowest single-particle energy state. The evaporation rate is suppressed by a factor $\exp(-\eta)$ where typically $\eta \sim 10$ and, as the gas cools down, the trap depth is reduced to force further evaporation [9].

For a deeply degenerate Fermi gas, $T \ll T_F$, the evaporation rate is given by [9].

$$\Gamma_{\text{evap}} \propto \gamma_{\text{coll}} \frac{T}{T_F} \exp \left[-\frac{U_{\text{trap}} - k_B T_F}{k_B T} \right] \quad (26)$$

where γ_{coll} is the classical collision rate evaluated at the Fermi surface. This can also be written as

$$\Gamma_{\text{evap}} \propto \gamma_{\text{coll}} \frac{T}{T_F} \exp \left[\frac{1}{T/T_F} \right] \exp \left[-\frac{1}{T/T_F} \left(\frac{U_{\text{trap}}}{k_B T_F} \right) \right] \quad (27)$$

We define $\eta_F \equiv U_{\text{trap}}/k_B T_F$ and observe that

$$\Gamma_{\text{evap}} \propto \gamma_{\text{coll}} \frac{T}{T_F} \exp \left[-\frac{\eta_F - 1}{T/T_F} \right] \quad (28)$$

We see that for a given value of T/T_F , the evaporation rate depends only on η_F . The effective η factor which determines the exponential suppression of the evaporation due to the trap depth is given by

$$\exp(-\eta_{\text{eff}}) = \frac{T}{T_F} \exp \left[-\frac{\eta_F - 1}{T/T_F} \right] \quad (29)$$

Besides the Boltzmann exponential suppression, the evaporation rate is additionally suppressed by a factor T/T_F due to Pauli blocking of one of the final states of a collision, which occurs for $T \ll T_F$ [9]. For a value of $T/T_F = 0.1$ to get $\eta_{\text{eff}} = 10$ we need $\eta_F = 1.77$

Lattice potential This line shows a representation of the modulation produced by the lattice potential. The period of the modulations shown is arbitrary and only for illustration purposes. A thin line is also plotted showing the envelope of the lattice potential.

Trap profiles of thermodynamic quantities. The smaller plot on the top left corner on Fig. 6 shows the trap profiles of the thermodynamic quantities. It includes the density (d), double occupancy (d), entropy per lattice site (s_L) and entropy per particle (s_N). The entropy per particle is shown on the right side axis.

Overall values of the thermodynamic quantities. The labels on the top left of the the smaller plot indicate the overall trap values of the thermodynamic quantities that can be obtained by integrating the local values across the volume of the trap.

Now that we have explained the relevant profiles and quantities that can be calculated from the LDA we will use it to get some insight on the idea of entropy redistribution, the possibility of evaporative cooling in the lattice and the optimal design parameters for the comp LATT

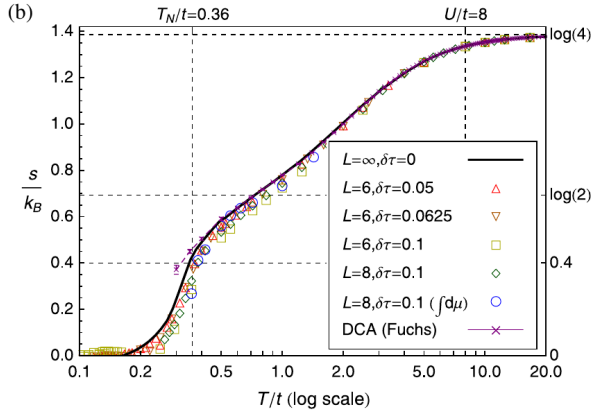


FIG. 1 (color online). (a) Energy per site of homogeneous system at half filling and $U/t = 8$, calculated by using DQMC down to $T/t = 0.1$. Statistical error bars are smaller than symbols. The solid curve is the entropy extrapolated to $L = \infty$ and $d\tau = 0$ (details in Ref. [11]). (b) Entropy per site obtained by integrating down from $T = \infty$, showing a shoulder at the Mott scale $T_{\text{Mott}} \approx U$ and a distinct feature at the Néel temperature $T_N \approx 0.36t$ due to critical fluctuations. Errors in E/t and s/k_B are both about 0.02. Our extrapolated results are fully consistent, within error bars, with the DCA results from Fuchs *et al.* [6].

(a) Paiva [5]

Figure 9: Calculations of entropy per lattice site versus temperature at half filling.

3.1 Entropy redistribution

In the quest for producing an antiferromagnetically (AFM) ordered state with cold atoms, the entropy per particle, S/N , is an important metric. It determines the number of quantum states that are accessible to each atom. At half-filling there is an average of one-particle per site². If the temperature of the system is high, $T \gg U$, there is an equal probability for a site to be empty, singly or doubly occupied. If the site is singly occupied, the spin there could be up or down, so at high temperatures there are a total of four ($|0\rangle, |\uparrow\rangle, |\downarrow\rangle, |\uparrow\downarrow\rangle$) equally probable state at each lattice site, giving an entropy per particle³ ~~is~~ equal to $s/k_B = \ln 4 = 1.38$.

When the temperature is $T \ll U$, double occupancies and vacancies are suppressed and the system enters the Mott insulating state. In this case the probability of having empty sites or doubly occupied sites goes to zero. At each site, a particle can still be spin-up or spin-down with equal probability, so the entropy per particle becomes $s/k_B = \ln 2 = 0.69$.

As the temperature of the system goes below the Néel temperature, the spin of the atoms becomes strongly determined by their position in the lattice, as they start to order antiferromagnetically. At zero temperature each site has only one possible quantum state (spin-up or spin-down depending on the lattice site) and the entropy per particle goes to zero.

For a homogeneous 3D lattice, at the Néel temperature $T_N = 0.36t$, the entropy per particle is $s = 0.4 k_B$. As the temperature starts dropping below T_N the entropy approaches zero very quickly in what is referred to as the AFM transition (AFM stands for antiferromagnetic order). The AFM transition has

²Notice that half-filling corresponds to $n = 1$, for this reason sometimes the terms half-filling, unit filling, and unit density are used interchangeably. Here we will restrict the terminology to half-filling or we will write explicitly $n = 1$ to avoid confusion.

³Notice that at half-filling any quantity per particle is the same as per lattice site, since $n = 1$

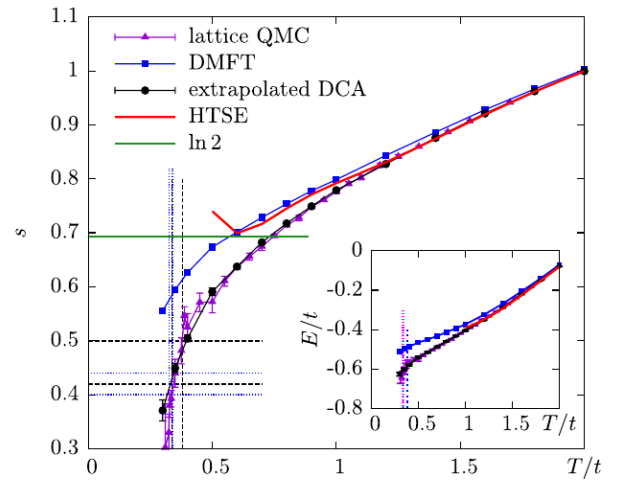


FIG. 1 (color online). Entropy per lattice site s of the Hubbard model as a function of temperature T/t , for $U/t = 8$, at half filling. Dashed vertical lines (black): T_N from Ref. [20]; dotted lines (blue): according to DMC simulations. Dashed horizontal lines (black): entropy per lattice site s at T_N [20]; dotted lines (blue): according to DMC simulations; $\log(2)$ is shown as a solid (green) horizontal line. Inset: Energy E/t per lattice site. The DMC data were extrapolated linearly in $1/L$ from the data at $L = 6, 8, 10$.

(b) Fuchs [6]

Figure 9: Calculations of entropy per lattice site versus temperature at half filling.

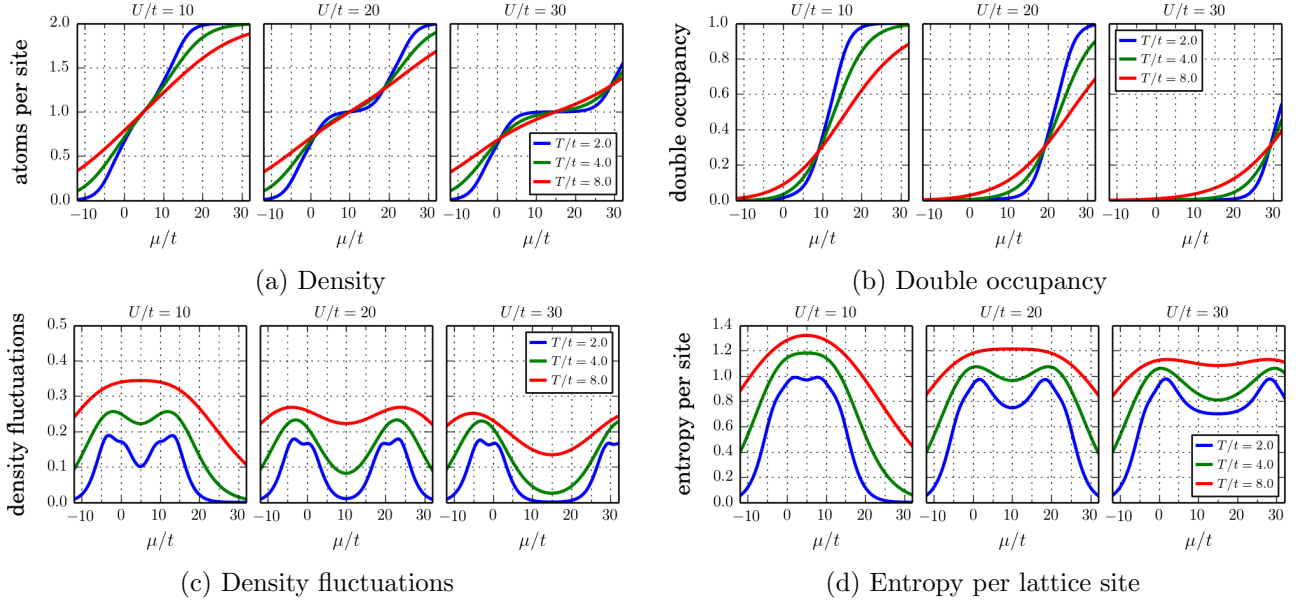


Figure 10: Thermodynamic quantities as a function of chemical potential calculated using the HTSE.

been studied theoretically for homogeneous 3D systems using quantum Monte Carlo (QMC) [5] and the dynamical cluster approximation (DCA) [6]. The results from these two approaches are shown in Figs. 9a,9b.

The theoretical calculations shown correspond to a homogeneous system, but in practice one has samples with a finite number of atoms so one is forced to confine them in order to reach half-filling. Since the confinement is typically harmonic (as opposed to a well with hard walls), the density decays as a function of distance to the center. This inhomogeneity in the density leads to the concept of entropy redistribution. As a consequence, the overall entropy per particle necessary to achieve a Néel state can be higher in a trapped system than in the homogeneous case. *[THREE-TA]*

3.1.1 High temperature series expansion for the Hubbard model

The high temperature series expansion (HTSE) to second order [7, 3] allows us to visualize the properties of the Hubbard model. It works well to capture the properties of the Mott insulating state, however it fails below temperatures of $T/t \approx 1.8$, so the AFM state is out of reach for HTSE. *[HS graph]*

The signatures of the Mott insulating states can be seen in the HTSE solutions shown in Fig. 10. Namely:

- The density as function of chemical potential has a plateau at $n = 1$, Fig. 10a.
- The double occupancy is suppressed for lower temperatures, Fig. 10b.
- The density fluctuations are suppressed, Fig. 10c.
- The entropy per site as a function of filling has a dip at $n = 1$, Fig. 10d.

3.1.2 Entropy per particle

The HTSE gives us the result for the entropy per lattice site, which we can plot versus the density, as shown in Fig. 11. The interesting result arises if we divide the entropy per lattice site by the density, in

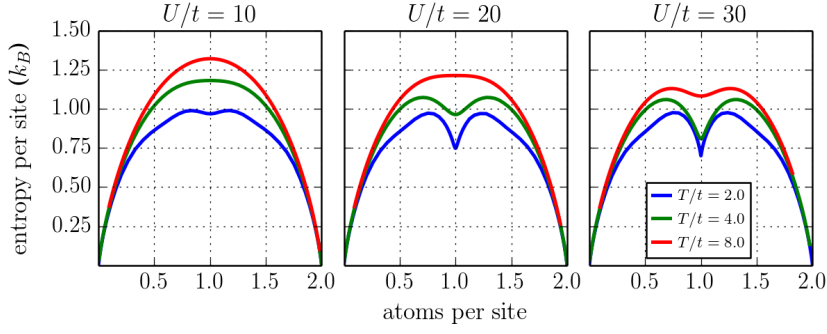


Figure 11: Entropy per lattice site versus density.

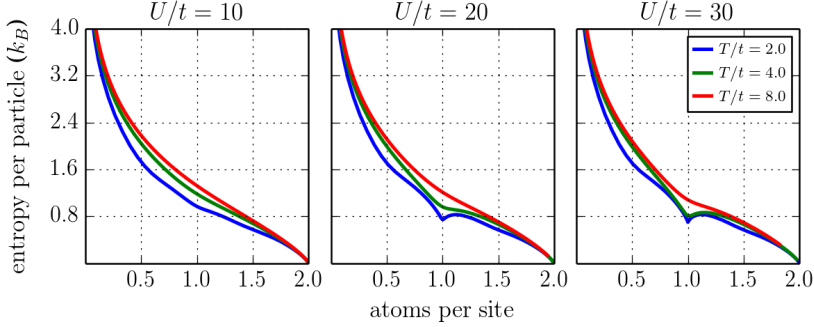


Figure 12: Entropy per particle versus density.

order to obtain the entropy per particle. This is shown in Fig. 12. It is seen there that the entropy per particle rises significantly for lower filling values, and most importantly that the value of the entropy per particle at low filling **does not** depend strongly on temperature or interaction strength. This property is referred to as the larger entropy capacity of the metallic shell, which is at the root of the idea of entropy redistribution.

In a finite trapped system which inevitably has a shell with density n_{cl} , a large part of the total entropy of the system is carried by the shell, allowing the core to be at an effectively lower entropy per particle. At a lower local entropy per particle the core can enter the AFM state even if the overall value of S/μ for the entire trap is larger than the Néel entropy of $S/\mu = 0.4k_B$ obtained for the homogeneous Hubbard model.

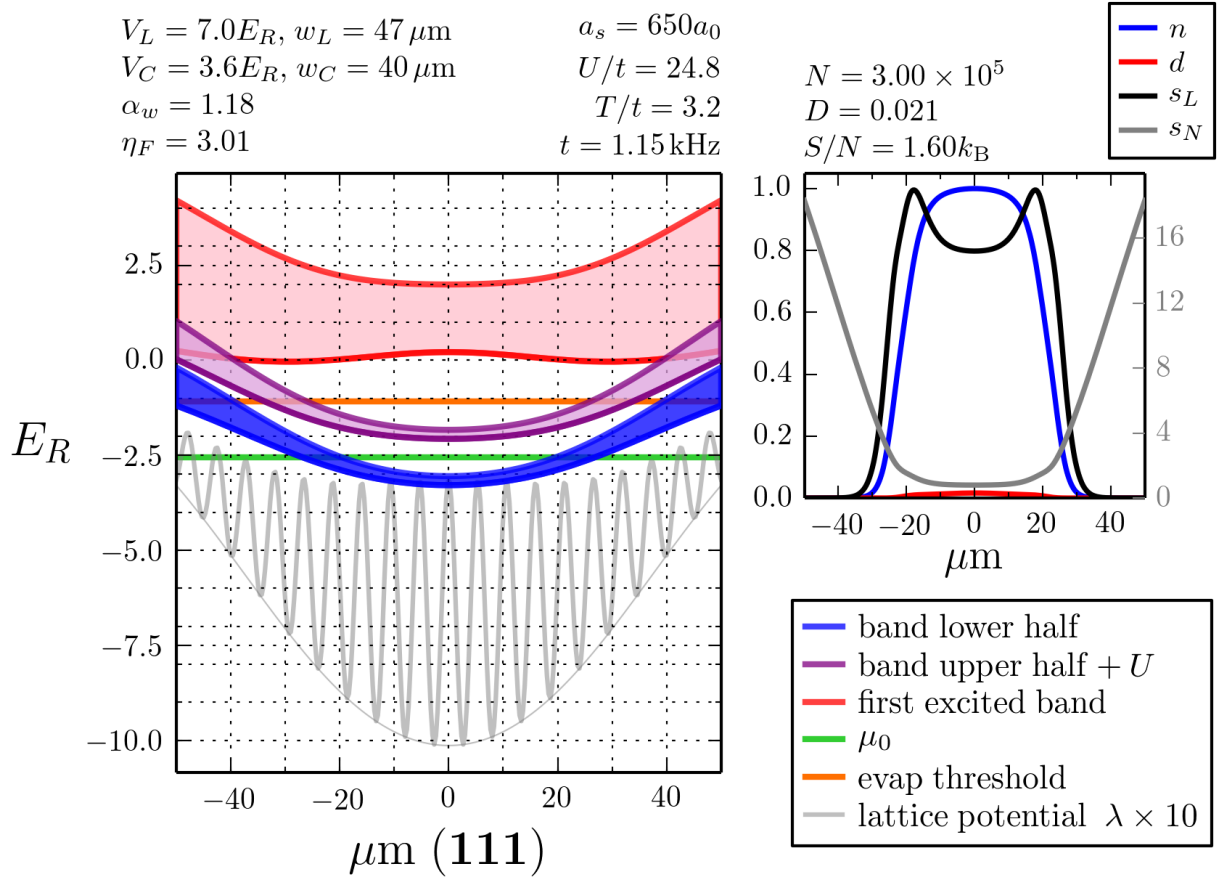


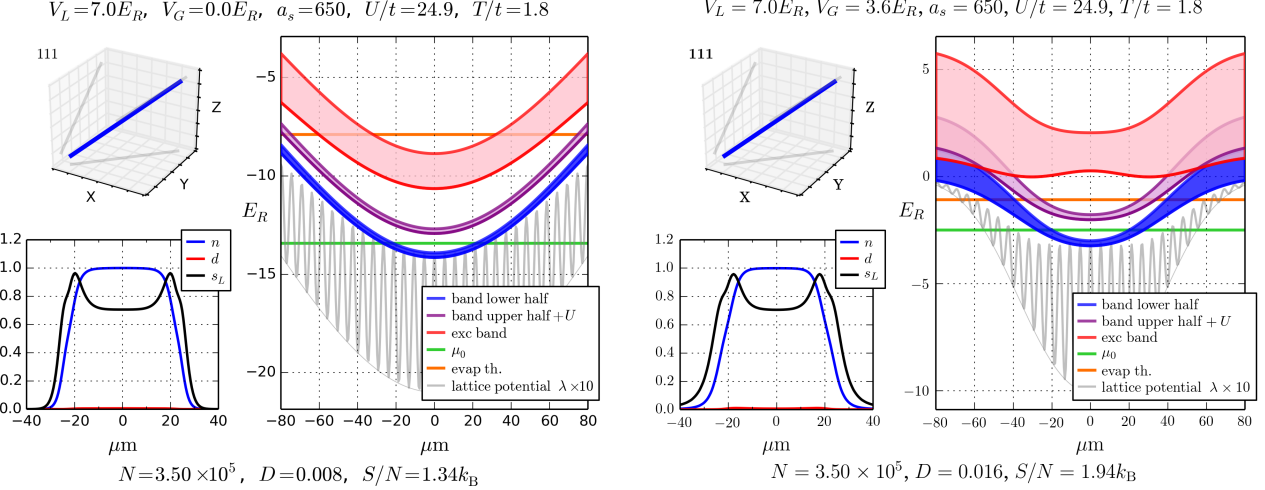
Figure 13: Red detuned lattice with compensation. The lattice beam waist is $47 \mu\text{m}$ and the compensation beam waist is $40 \mu\text{m}$. These values are approximately what we use in our experimental setup. The compensation depth of $3.6 E_R$ is chosen so that unit filling is achieved at the center for an atom number of 350,000.

3.2 Local density approximation

In what follows we will use the results from HTSE and the local density approximation to calculate trap profiles of the various thermodynamic quantities. A trapped gas with a finite number of atoms has a density that inevitably decreases as a function of distance from the center. As the density goes down, the outer shells of the cloud, which are below half-filling, will have a large entropy per particle. The overall entropy per particle of the trapped system, S/N , will be distributed such that most of it is carried by the metallic edges of the cloud.

3.2.1 Comparison between a red detuned lattice without and with compensation

Figure 14 shows a comparison of the trap profiles for a red detuned lattice without compensation (14a) and a red detuned lattice with compensation (14b). In order to make a legitimate comparison, we set the atom number to 350,000 atoms. In the case without compensation we vary the beam waist of the lattice beams such that a density of $n = 1$ is achieved at the center of the sample. Lattice beams with smaller beam waists will produce a stronger confinement, so in general if you have a large amount of atoms and you want to achieve unit filling without compensation you must use lattice beams with a large waist. In the case with compensation we use the lattice and compensation beam waists that we currently have



(a) Red detuned lattice without compensation. The lattice beam waist is $146\mu\text{m}$ for all three lattice axes. The beam waist is chosen such that the confinement produces unit filling at the center when there are 350,000 atoms in the trap.

(b) Red detuned lattice with compensation. The lattice beam waist is $47\mu\text{m}$ and the compensation beam waist is $40\mu\text{m}$. These values are approximately what we use in our experimental setup. The compensation depth of $3.6E_R$ is chosen so that unit filling is achieved at the center for an atom number of 350,000.

Figure 14: Full trap profiles of band structure and thermodynamic quantities for a lattice without and with compensation. For both cases the atom number is chosen to be 350,000 atoms, and the filling at the center is $n = 1$. Note that despite the very different band structure profiles, the density profiles are very similar for both cases. Even though the local Hubbard parameters and the filling are set to be the same at the center of the sample, the overall entropy per particle can be 1.5 times larger in the compensated case ($1.94k_B$) than in the uncompensated case ($1.34k_B$).

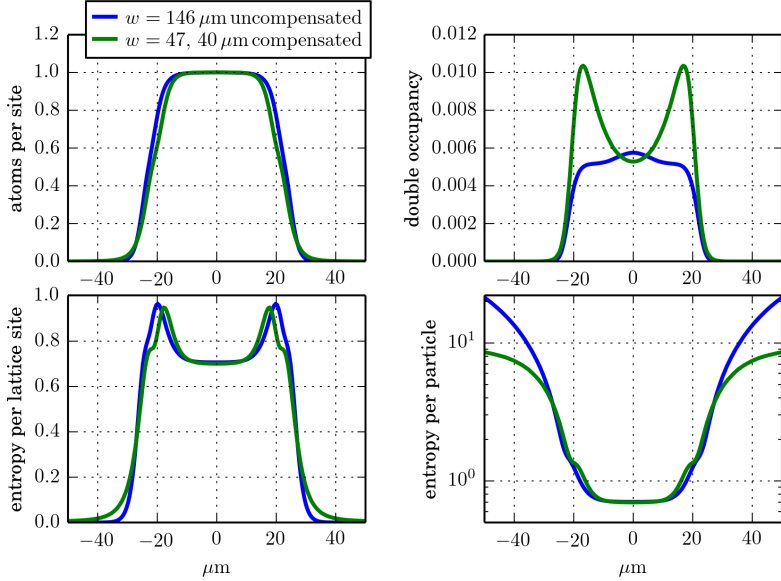


Figure 15: Detailed comparison of the thermodynamic quantities for the large beam waist uncompensated lattice and the small beam waist compensated lattice. The density is very similar for both cases. The double occupancy is quite different, which leads to a very slightly larger entropy per particle across a large range of radii in the trap.

in our setup: $w_L = 47 \mu\text{m}$ and $w_C = 40 \mu\text{m}$. We then adjust the depth of the compensation beams to achieve half filling with 350,000 atoms.

From looking at this figure we can see that even though the band structure profiles are very different (in the compensated case the Hubbard parameters vary strongly with radial distance), the trap profiles of the density look very similar in both cases. Despite this similarity in the density, the double occupancy and the entropy per lattice site are slightly different. The important result is that even though in both cases one has the exact same local state at the center (same filling, same U/t , same s) the overall entropy per particle can be larger for the compensated lattice by a factor of 1.5 (1.94 k_{B} to 1.34 k_{B}).

This larger capacity of the compensated lattice to redistribute entropy is what can make it favorable to achieve an AFM ordered state at the center of the sample. If one looks in more detail, as is shown in Fig. 15 one realizes that the larger entropy capacity comes from a small enhancement of the double occupancy (on the half-a percent level) which leads to a slightly larger entropy per particle on the region from about 5 μm to 25 μm radius. This radii encompass a large volume of the trap, which can make a difference on the overall entropy capacity even though the extra entropy per particle plotted radially looks very small.

The profiles that are shown in Fig. 14 are calculated at a temperature $T = 1.8t$, which is near the lowest temperature value accessible with the HTSE. The chemical potential, measured from the lowest energy level available to the system (the bottom of the band) is set to $\mu = 6t + U/2$ to guarantee half-filling at the center.⁴ We used a value of $U = 24.9t$, given by the scattering length, which is set at $650a_0$.

Plugging in these values we obtain $\mu \approx 18t$ or $T/\mu \approx 1.8/18 = 0.1$. When the temperature is so low, one can safely assume that $\mu \approx E_F$, so this system would have $T/T_F = 0.06$ at an overall entropy per particle of $S/N = 1.94k_{\text{B}}$. If the sample was obtained by ramping up the lattice adiabatically starting

⁴The $6t$ here is half the bandwidth. Note that in typical treatments the chemical potential is always measured from the center of the lowest band, so the $6t$ will be omitted. In that case the chemical potential associated with half-filling Will be $U/2$. Some treatments even shift the zero of energy by $U/2$ so that half filling occurs nominally at $\mu=0$ regardless of U .

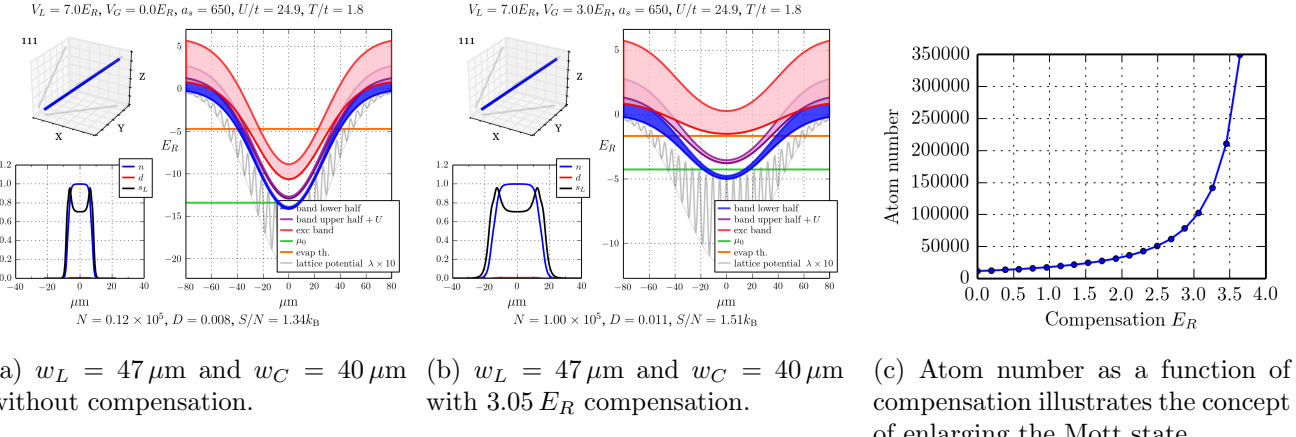


Figure 16: Illustrating the idea of enlarging the Mott state.

from a harmonic trap, then the initial entropy in the harmonic trap should also be $1.94k_{\text{B}}$. In the harmonic trap this corresponds to $T/T_F = S/(\pi^2 N) \approx 0.2$.

We conclude from these rough estimates that as the sample gets loaded into the lattice it gets adiabatically cooled, its value of T/T_F is reduced. This is in contrast with the result obtained in [8] where it was concluded that loading a gas adiabatically from a harmonic trap to a deep optical lattice would adiabatically heat the gas. In this case we are considering interactions and not neglecting the width of the lowest band. Our observation that the gas is adiabatically cooled as it is loaded into the lattice are consistent with the results from [5].

(NOTE: I NEED TO ASK THEREZA ABOUT THESE REMARKS TO CHECK THAT I AM NOT MAKING A MISTAKE.

The main question is whether it is ok to take $\mu = E_F$ since μ is in the Mott gap. Should one take $E_F = 12t$ in that case, since the top of the band is the largest energy state that could potentially be occupied??)

3.2.2 Enlarging the Mott state

In this section we consider our experimental setup ($w_L = 47 \mu\text{m}$, $w_C = 40 \mu\text{m}$) and we vary the amount of compensation. What we find is that if no compensation is used, then the number of atoms has to be very small in order to achieve half-filling at the center. On the other hand, when using compensation one can still hold a large number of atoms and maintain half-filling. This leads to the concept of enlarging the Mott state (or Néel state if your temperature is low enough) which can be a very dramatic effect as was shown in the paper by Mathy, Huse and Hulet [4].

The effect of enlarging the Mott state is shown in Fig. 16, where we show the relationship between atom number and compensation when the filling is set to $n = 1$ at the center of the cloud. This figure also shows the profile plots for no compensation and a compensation of $3.05 E_R$, in order to illustrate how the Mott plateau in the density profile is enlarged for larger compensation.

From what was discussed in §3.2.1 we see that it is also possible to reach an large Mott plateau for $N = 350,000$ and without compensation beams: you just need to have larger lattice beam waists. As we saw there, the advantage of realizing the large Mott plateau with small lattice beam waists and compensating beams is that this system has a larger entropy capacity than the large-beam-waist-uncompensated counterpart.

In addition to this entropy capacity advantage, the small-beam-waist-compensated setup offers the possibility of evaporative cooling since the chemical potential comes much closer to the energy threshold for an atom escaping along one of the lattice beams. We will address this point in the following section.

4 Evaporative cooling in a lattice

If we refer back to Fig. 14 we can see that on the energy landscape plot we used an orange line to indicate the evaporation threshold, that is the energy necessary for an atom to escape along one of the lattice beams. Comparing the two cases one sees that the small beam waist compensated case has a global chemical potential (green line) that is much closer to the evaporation threshold.

When evaporative cooling a thermal gas of atoms, one considers the parameter $\eta = U_{\text{trap}}/k_B T$, where U_{trap} is the energy threshold for a particle leaving the trap (i.e. the trap depth) and T is the temperature of the gas. The evaporation rate is suppressed by a factor $\exp(-\eta)$ where typically $\eta \sim 10$ and, as the gas cools down, the trap depth is reduced to force further evaporation [9].

For a deeply degenerate Fermi gas, $T \ll T_F$, the evaporation rate is given by [9].

$$\Gamma_{\text{evap}} \propto \gamma_{\text{coll}} \frac{T}{T_F} \exp \left[-\frac{U_{\text{trap}} - k_B T_F}{k_B T} \right] \quad (30)$$

where γ_{coll} is the classical collision rate evaluated at the Fermi surface. This can also be written as

$$\Gamma_{\text{evap}} \propto \gamma_{\text{coll}} \frac{T}{T_F} \exp \left[\frac{1}{T/T_F} \right] \exp \left[-\frac{1}{T/T_F} \left(\frac{U_{\text{trap}}}{k_B T_F} \right) \right] \quad (31)$$

We define $\eta_F \equiv U_{\text{trap}}/k_B T_F$ and observe that

$$\Gamma_{\text{evap}} \propto \gamma_{\text{coll}} \frac{T}{T_F} \exp \left[-\frac{\eta_F - 1}{T/T_F} \right] \quad (32)$$

For the deeply degenerate gas, the η factor which determines the exponential suppression of the evaporation due to the trap depth is effectively

$$\eta = \frac{\eta_F - 1}{T/T_F} \quad (33)$$

Notice that the evaporation rate is additionally suppressed by a factor T/T_F due to Pauli blocking of one of the final states of a collision, which occurs for $T \ll T_F$ [9].

We start by considering a red-detuned lattice with no extra confinement or compensation. We set $n = 1$ at the center of the sample and vary the waist of the lattice beams. From our knowledge of the potentials we can determine U_{trap} , which in this case is the energy required for an atom to escape along one of the lattice beams. At a temperature of $T = 1.8t$ we can make the approximation $k_B T_F \approx \mu$, where μ is the global chemical potential. Figure 17 shows η_F as a function of lattice beam waist, and also shows the number of atoms required to achieve half-filling.

In our experiment we can produce cold samples with $\sim 350,000$ atoms. As can be seen in Fig. 17 (and also was already shown in Fig. 14a), using a beam waist of $146 \mu\text{m}$ would produce the confinement necessary to reach half-filling at the center with $N = 350,000$. The flip side of this is that, for that beam waist η_F would be ≈ 8.5 , which for $T/T_F = 0.1$ means that the rate of evaporation would be

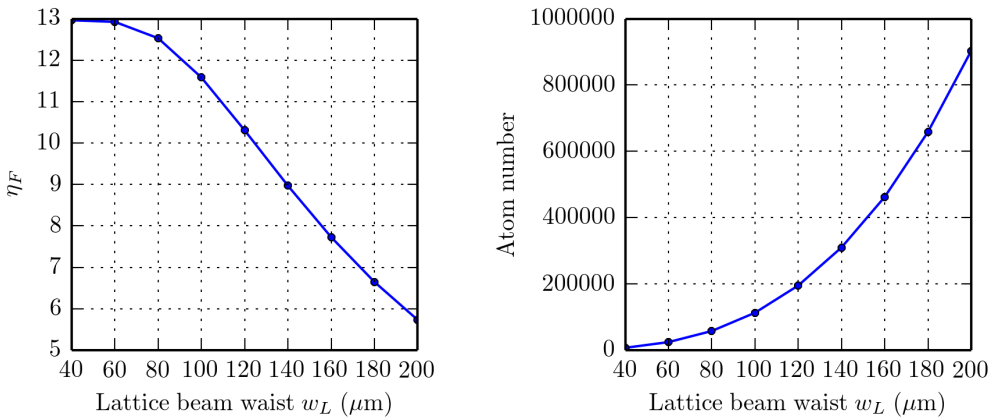


Figure 17: η_F , an indicator of the exponential suppression of evaporation is shown as a function of lattice beam waist for a red-detuned lattice without any extra confinement or compensation. To determine η_F the number of atoms is adjusted such that filling is $n = 1$ at the center. The required number is shown on the right.

suppressed by

$$\frac{T}{T_F} \exp \left[-\frac{\eta_F - 1}{T/T_F} \right] \equiv \xi_{\text{evap}} \approx 10^{-34} \quad (34)$$

Going back to our current setup, which has $w_L = 47 \mu\text{m}$ and $w_C = 40 \mu\text{m}$, with 350,000 atoms; we can achieve half filling if we use $3.64E_R$ of compensation. This yields $\eta_F \approx 2.95$. This is a lot better than the large-beam-waist-uncompensated case, however the suppression factor for the rate of evaporative cooling is still very small. For our current setup it would be

$$\xi_{\text{evap}} = 3.4 \times 10^{-10} \quad (35)$$

Under typical evaporation conditions $\eta = 10$, and for a non-degenerate sample we have

$$\xi_{\text{evap}} = e^{-10} = 4.5 \times 10^{-5} \quad (36)$$

We conclude that our current setup would have an evaporation rate **five orders of magnitude smaller** compared to the typical evaporative cooling rate for a thermal gas (given the same rate of elastic collisions γ_{coll}). In addition, in order to get a more realistic estimate we would need to incorporate the implications of the chemical potential being in a gapped region of the spectrum (for half-filling the chemical potential is at the center of the Mott gap) which should further reduce the evaporation rate.

We now explore the entire parameter space, where we allow the lattice and compensation beam waists to vary. We set the chemical potential so that $n = 1$ at the center of the sample, we do this because half-filling is a prerequisite to achieve Mott or Néel states. We attempt to find a compensation such that $N = 350,000$ atoms. For some values of the beam waists that is not possible because it would lead to either spilling atoms from the trap⁵ or to the creation of a negative curvature in the confinement at the center of our sample⁶.

The results of the exploration of the beam waist parameter space are shown in Fig. 18. The main points that stand out are

⁵In cases when $w_C > w_L$.

⁶In cases when $w_C < w_L$. We also refer to this as making a donut

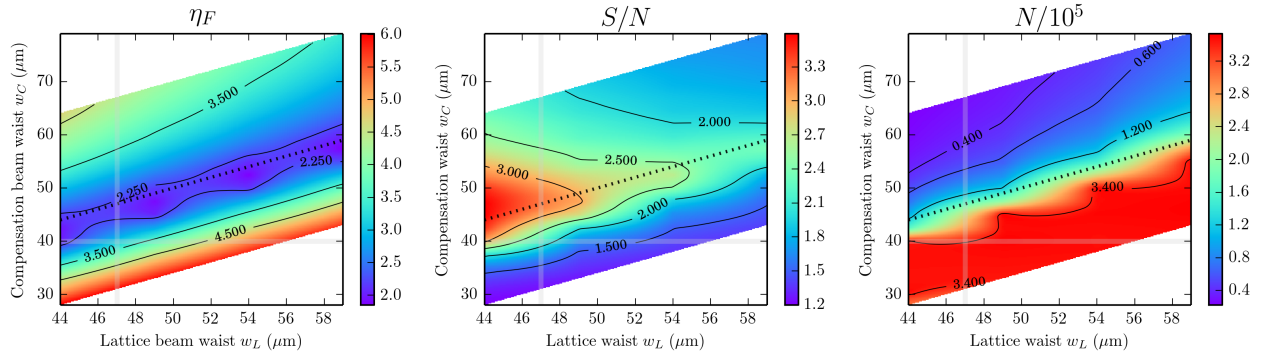


Figure 18: η_F and S/N and N are plotted for various lattice and compensation beam waists. The filling is set to $n = 1$ at the center. The compensation depth is adjusted so that $N = 350,000$ if it is possible, otherwise it is set to maximize the atom number without spilling any atoms form the trap or creating a Mexican hat at the center of the potential. The dotted line in the plots corresponds to $w_L = w_C$. The current values of our experimental setup are shown as gray lines, such that the intersection between these two gray lines represents our current conditions.

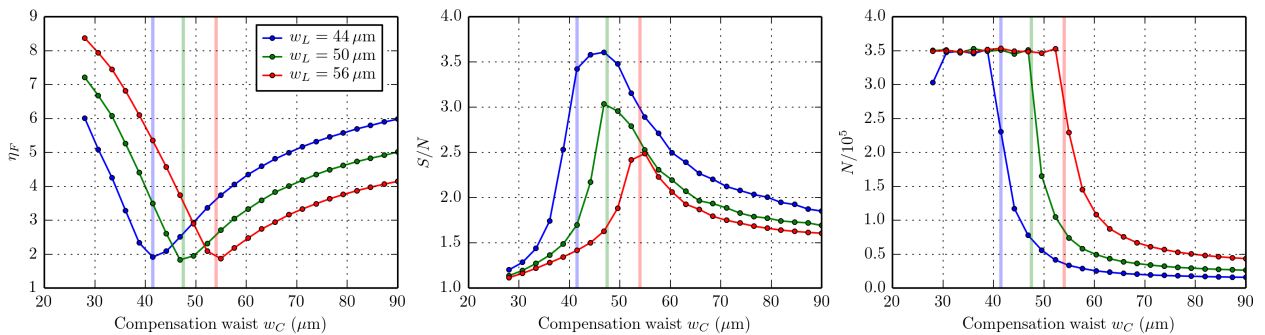


Figure 19: η_F , S/N , and N as a function of w_C for various values of w_L .

- An optimal value of η_F is achieved for $w_L \approx w_C$.
- At $w_L \approx w_C$, smaller beam waists give better entropy capacity
- The atom number can only reach 350,000 if $w_C < w_L$, such as in our current setup. Otherwise the atom number is limited, being smaller for larger w_C .

To get another look at the results, on Fig. 19 we plot η_F , S/N , and N as a function of w_C for three different values of w_L . The evaporation factor is optimized for nearly equal beam waists and the entropy capacity also peaks up around there. Given this observation, we now set $w_L = w_C$ and vary both together to see if it is favorable to make smaller or larger beam waists. This is shown in Fig. 20. The main observations are:

- For beam waists up to $\approx 68 \mu\text{m}$ one can keep getting lower η_F by making the beam waists larger. This trend would continue if we had an unlimited number of atoms, however beyond $\approx 68 \mu\text{m}$ the number of atoms required to fill the trap goes above our cap of 350,000 atoms.
- For larger beam waists the entropy capacity is always lower, so the choice of beam waist will be a compromise between η_F and the entropy capacity.

The results shown in Figs. 20, 19 show that it is desirable to have equal lattice and compensation beam waists. The choice of their value is a compromise between the achievable η_F and the entropy capacity,

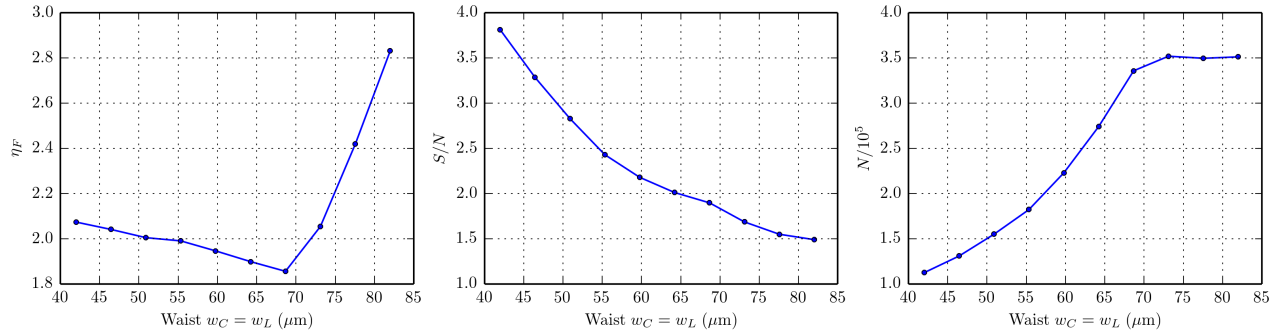


Figure 20: η_F and S/N as a function of beam waist for $w_L = w_C$. Results are shown for various atom numbers.

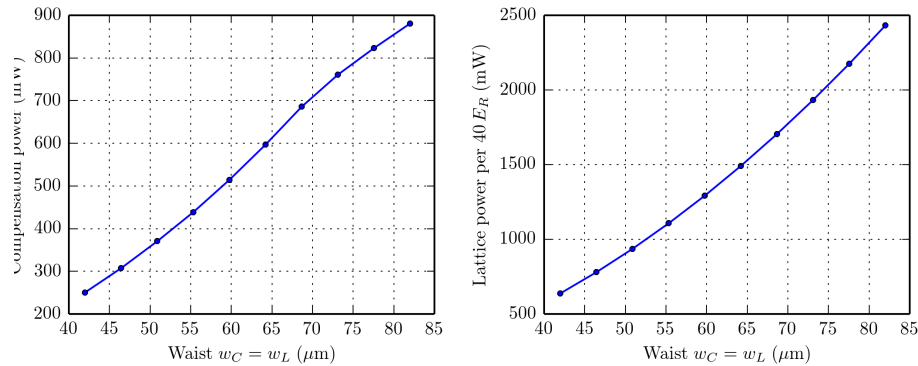


Figure 21: Compensation power required to compensate a $7 E_R$ lattice and lattice powered required to achieve a $40 E_R$ lattice depth.

given by S/N . Another important experimental constraint is the available of power at the lattice and compensation wavelengths, which is a bigger issue for larger beam waists. In that case larger power is necessary to achieve the required potential depths. The compensation power needed to compensate a $7 E_R$ lattice and the lattice power needed to make a $40 E_R$ deep lattice⁷ are shown in Fig. 21. With this in mind and our available powers we can safely realize any choice of beam waists below $65 \mu\text{m}$.

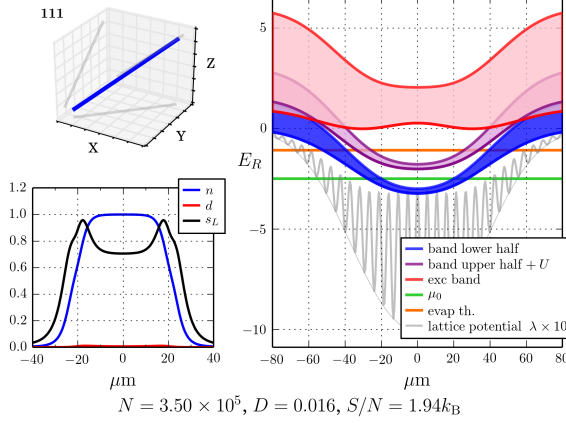
To fully exploit the atom number that we can produce in our experiment our opinion is to go to the larger lattice beam waists, so we recommend values of $w_L = w_C = 65 \mu\text{m}$. These proposed parameters would change the evaporation factor and entropy capacity and number capacity of our setup according to the following table:

	w_L (μm)	w_C (μm)	η_F	ξ_{evap}	S/N
Current setup	47	40	2.95	3.4×10^{-10}	1.94
Proposed change	65	65	1.52	1.36×10^{-5}	1.99

We see that for the optimal beam waist ratio a value of $\xi_{\text{evap}} \sim 10^{-5}$ may be reached that could lead to reasonable rates of evaporation in the lattice. A comparison of our current setup and this proposed scenario is shown in Fig. 22.

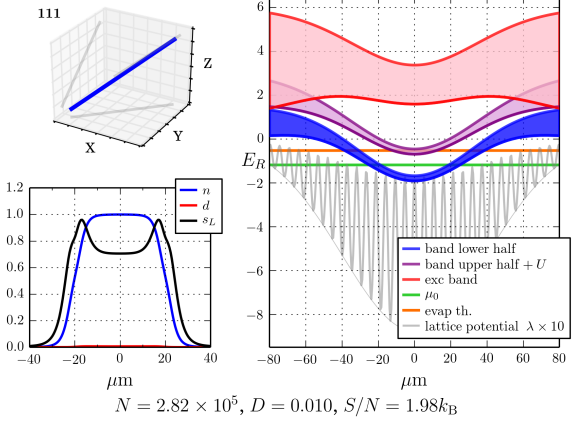
⁷If we want to freeze out tunneling in the lattice we required depths as large as $40 E_R$ where the tunneling rate goes down to 3 Hz. We currently “lock” the lattice at $20 E_R$ for our Bragg scattering measurements. At $20 E_R$ the tunneling rate is 72 Hz. This is good enough for Bragg scattering, but not good enough for measurements that take longer, such as associating through the narrow Feshbach resonance to measure double occupancies.

$$V_L = 7.0E_R, V_G = 3.6E_R, a_s = 650, U/t = 24.9, T/t = 1.8$$



(a) $w_L = 47 \mu\text{m}$ and $w_C = 40 \mu\text{m}$. Compensation is chosen so that unit filling is achieved at the center for an atom number of 350,000.

$$V_L = 7.0E_R, V_G = 4.1E_R, a_s = 650, U/t = 24.9, T/t = 1.8$$



(b) $w_L = 65 \mu\text{m}$ and $w_C = 65 \mu\text{m}$. Atom number maxes out at 284,000 atoms.

Figure 22: Full trap profiles of band structure and thermodynamic quantities for our current setup and the proposed setup with equal beam waists.

5 Conclusions

References

- [1] I. Bloch and W. Zwerger, “Many-body physics with ultracold gases,” *Reviews of Modern Physics* **80**, 885–964 (2008).
- [2] U. Schneider, Ph.D. thesis, Johannes Gutenberg - Universitat in Mainz, 2010.
- [3] R. Jördens, Ph.D. thesis, ETH Zürich, 2010.
- [4] C. J. M. Mathy, D. a. Huse, and R. G. Hulet, “Enlarging and cooling the Néel state in an optical lattice,” *Physical Review A* **86**, 023606 (2012).
- [5] T. Paiva, Y. L. Loh, M. Randeria, R. T. Scalettar, and N. Trivedi, “Fermions in 3D Optical Lattices: Cooling Protocol to Obtain Antiferromagnetism,” *Physical Review Letters* **107**, 086401 (2011).
- [6] S. Fuchs, E. Gull, L. Pollet, E. Buровски, E. Kozik, T. Pruschke, and M. Troyer, “Thermodynamics of the 3D Hubbard Model on Approaching the Néel Transition,” *Physical Review Letters* **106**, 030401 (2011).
- [7] J. Henderson, J. Oitmaa, and M. Ashley, “High-temperature expansion for the single-band Hubbard model,” *Physical Review B* **46**, 6328–6337 (1992).
- [8] M. Köhl, “Thermometry of fermionic atoms in an optical lattice,” *Physical Review A* **73**, 031601 (2006).
- [9] K. OHara, M. Gehm, S. Granade, and J. Thomas, “Scaling laws for evaporative cooling in time-dependent optical traps,” *Physical Review A* **64**, 051403 (2001).